THE JOURNAL OF PHYSICAL CHEMISTRY C

ARTICLE

pubs.acs.org/JPCC

Hollow Mesoporous Silica/Poly(L-lysine) Particles for Codelivery of Drug and Gene with Enzyme-Triggered Release Property

Yufang Zhu,*[,†] Wenjun Meng,[‡] Hong Gao,[§] and Nobutaka Hanagata[‡,⊥]

[†]School of Materials Science and Engineering, University of Shanghai for Science and Technology, 516 Jungong Road, Shanghai 200093, P. R. China

[‡]Graduate School of Life Science, Hokkaido University, N10W8, Kita-ku, Sapporo 060-0812, Japan

[§]International Center for Young Scientists, National Institute for Materials Science, 1-2-1 Sengen, Tsukuba, Ibaraki 305-0047, Japan

[⊥]Interdisciplinary Laboratory for Nanoscale Science and Technology, National Institute for Materials Science, 1-2-1 Sengen, Tsukuba, Ibaraki 305-0047, Japan

Supporting Information

ABSTRACT: We designed, for the first time, an enzyme-triggered drug and gene codelivery system combining hollow mesoporous silica (HMS) with enzyme degradable poly(L-lysine) (PLL) polymer to form HMS/PLL particles driven by electrostatic interaction between negatively charged gene and positively charged PLL polymer on the drug-loaded HMS particles. Fluorescein and cytosine−phosphodiester−guanine oligodeoxynucleotide (CpG ODN) were used as the model drug and gene, and the loading and the layer-by-layer assembly were evaluated by UV/vis analysis, zeta potential measurement, and gel electrophoresis. The fluorescein and CpG ODN loading capacities of the MFHMS/$(CpG/PLL)_3$ particles were 28.8 and 97.1 μg/mg, respectively. Importantly, *in vitro* release results showed that the MFHMS/$(CpG/PLL)_3$ particles exhibited an enzyme-triggered controlled release of fluorescein and CpG ODN simultaneously in the α-chymotrypsin solution, and the release rates of fluorescein and CpG ODN could also be controlled by changing the enzyme concentration. Therefore, this system has the advantages of both enzyme-triggered controlled release and codelivery of drug and gene and would have potential and promising applications in the field of biomedicine and cancer therapy.

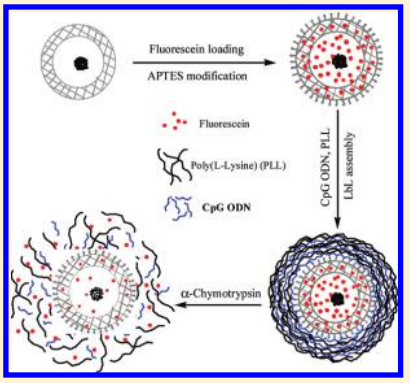

INTRODUCTION

Mesoporous silica nanoparticles (MSNs) for drug delivery system have drawn growing interest in the past decade. As result of their large surface area and pore volume, tunable mesopore size, biocompatibility, and the ease of surface functionalization, MSNs could serve as ideal inorganic carriers for drugs, proteins, and genes and deliver them to target sites.[1−4] Recently, many efforts have been made to pursue the MSNs-based stimuli-responsive controlled release systems[5−17] because stimuli-responsive controlled release could reduce the serious side effects associated with many drugs and enhance the therapeutic efficacy.[18] Various components, such as Au, Fe_3O_4, and CdS nanoparticles,[5−7] collagen,[8] oligonucleotide,[9,10] antibody,[11] supermolecules,[12] polyelectrolyte,[13] and coumarin,[14] have been employed to construct the gated MSNs for controlled drug release that respond to a range of stimuli including redox, pH or temperature, competitive binding, photoirradiation, and so on. However, many of the reported systems have the gating features in nonaqueous solvents, poor biocompatibility, toxicity of the gating agents, or difficulty for using under physiological conditions. In addition to the stimuli mentioned above, the use of enzymes is of great interest for triggering a responsive controlled drug release from a gated MSNs-based delivery system. Enzymes offer key advantages as release triggers because they are not biologically disruptive, function under mild conditions, and possess a high degree of selectivity.[19−22] To date, several reports on the use of enzyme-mediated hydrolysis for the controlled opening of the gated MSNs have been described.[23−28] For example, Patel et al. functionalized the external surface with a [2]rotaxane to cap the openings of the dye-loaded MSNs by an ester-linked adamantyl stopper, and the system showed "zero release" until the addition of porcine liver esterase that induced dethreading of the [2]rotaxane owing to hydrolysis of the adamantyl ester.[23] Bernardos et al. reported the synthesis of a lactose-capped MSNs for controlled release.[25] The $[Ru(bipy)_3]^{2+}$ dye could release from the lactose-capped MSNs after the addition of β-D-galactosidase to uncap the openings by the rupture of a glycosidic bond.[25] Despite some recent reported gated MSNs can be triggered for controlled drug release using enzymes, redox, or other stimuli, the approach of using the gated MSNs for the development of the drug delivery systems is still an incipient area of research.

Received: April 13, 2011
Revised: June 12, 2011
Published: June 15, 2011

On the other hand, codelivery of drugs and genes has been proposed to enhance gene expression to reduce drug resistance or to achieve a synergistic effect of drug and gene therapies, which may offer new opportunities in the area of cancer therapy.[29,30] Recently, many attempts have been made to develop the suitable carriers for the efficient codelivery of drugs and genes, such as liposomes, micellar nanoparticles, biodegradable copolymer, and graphene.[31−36] However, the studies on MSNs as carriers for codelivery of drug and gene are scant, although MSNs could serve as ideal carriers for drugs, proteins, and genes. To our knowledge, only two examples that involved the concept of codelivery of drug and gene using MCM-41 MSNs have been described.[37,38] Torney et al. reported, for the first time, codelivery of DNA and chemicals into plants using MSNs. They loaded MCM-41 MSNs with plasmid DNA and fluorescein and capped the ends with gold nanoparticles to keep the molecules from leaching out and uncapped the gold nanoparticles using a disulfide-reducing antioxidant, dithiothreitol (DTT), to trigger fluorescein release and gene expression in the plants.[37] Chen et al. developed a MCM-41 MSNs-based codelivery system (doxorubicin and Bcl-2 siRNA) by a similar strategy to enhance the efficacy of chemotherapy in multidrug-resistant cancer cells. In this case, generation 2 amine-terminated polyamidoamine (PAMAM) dendrimers and glutathione were used as the end-capping and stimuli, respectively.[38] Obviously, MSNs carriers have potential for codelivery of drugs and genes, but it is still challenging to develop more efficient strategies to simultaneously load and deliver drugs and genes.

It has been demonstrated that hollow mesoporous silica (HMS) particles exhibit a much higher drug loading capacity compared to the conventional mesoporous silica materials due to their large hollow cavities for drug storage.[39−42] On the other hand, poly(L-lysine) (PLL) polymers are polypeptides with amino acid lysine as a repeat unit and biodegradable. They are one of the first cationic polymers used for gene transfer due to their low immunogenicity, the capacity to deliver large DNA payloads, stability, and ease of the passage of DNA molecules through a cell membrane.[43,44] Furthermore, PLL polymers possessing enzymatic degradability facilitate DNA controlled release.[45,46] Therefore, it can be imagined that the combination of HMS particles and PLL polymers as carriers could realize the high loading capacity and enzyme-triggered controlled release of drug and gene simultaneously, which would be a potential and promising strategy to design a stimuli-responsive codelivery system of drug and gene.

Herein, we report, for the first time, the design and construction of an enzyme-responsive carrier for codelivery of drug and gene using HMS/PLL particles. As shown in Figure 1, the first step involves the loading of fluorescein, a model drug, into HMS particles and the modification with 3-aminopropyltriethoxysilane (APTES: $(C_2H_5O)_3SiCH_2CH_2CH_2NH_2$) on the surface of the fluorescein-loaded particles to obtain the modified fluorescein-loaded HMS (MFHMS) particles. In the next step, the MFHMS particles are coated by a layer-by-layer (LbL) assembly with negatively charged CpG ODN, a model gene, and positively charged PLL polymer alternatively to obtain the fluorescein and CpG ODN-loaded HMS/PLL particles (MFHMS/$(CpG/PLL)_n$, n is the assembled number). Finally, fluorescein and CpG ODN can simultaneously release from the MFHMS/$(CpG/PLL)_n$ particles stimulated by α-chymotrypsin that can induce PLL polymer degradation. Reports on such HMS/PLL particles for codelivery of drug and gene with enzyme-triggered release property have not been found before.

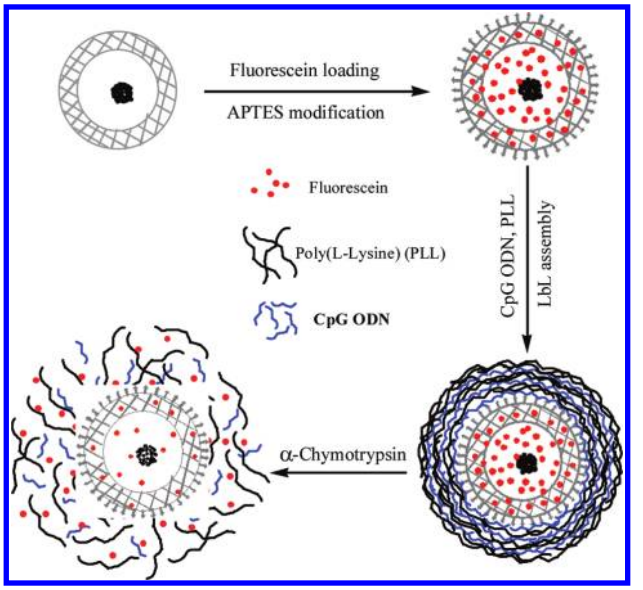

Figure 1. Schematic procedure for preparation of the fluorescein and CpG ODN-loaded HMS/PLL particles and enzyme-triggered release.

EXPERIMENTAL SECTION

Preparation of the Modified Fluorescein-Loaded HMS Particles (MFHMS). First, HMS particles were synthesized by the carbon spheres templating according to our previous reported method with some changes of synthesis parameters[47] (see Supporting Information). The MFHMS particles were prepared following the literature procedures after some modification.[9] 500 mg of HMS particles and 34.4 mg of fluorescein were suspended in 50 mL of anhydrous ethanol inside a sealed bottle. Then, the mixture was stirred for 24 h at 37 °C with the aim of achieving maximum loading in the cores and pores of HMS particles. Afterward, an excess of 3-aminopropyltriethoxysilane (1.5 mL, Aldrich) was added, and the suspension was stirred for 24 h. Finally, the yellow product (MFHMS) was centrifuged, washed with ethanol, and dried at 70 °C for 12 h.

Preparation of the Fluorescein and CpG ODN-Loaded HMS/PLL Particles (MFHMS/$(CpG/PLL)_n$). Natural phosphodiester (PD) CpG ODN 2006 (sequence: 5′-TCGTCGTTTT GTCGTTTTGTCGTT-3′) was diluted in sterilized water to a concentration of 1 μg/μL and stored at −20 °C until use. CpG ODN loading and PLL polymer coating were used by a layer-by-layer assembly. Typically, 20 μL of CpG ODN was added to 200 μL of the MFHMS suspension (1 μg/μL), and the resulting mixture was continuously shaken at 4 °C for 2 h, followed by centrifugation and washing with water for five times to remove the residual free dye and CpG ODN. Next, the MFHMS/CpG particles were immersed into 200 μL of positively charged PLL polymer solution (1.0 mg/mL in 0.5 M NaCl) for 30 min with shaking. The excess PLL polymer was removed by wash with water for five times. The same procedure was repeated to obtain the fluorescein and CpG ODN-loaded HMS/PLL particles (MFHMS/$(CpG/PLL)_n$).

***In Vitro* Release Behavior of the MFHMS/$(CpG/PLL)_n$ Particles.** *In vitro* release of fluorescein and CpG ODN from the MFHMS/$(CpG/PLL)_n$ particles was carried out with a shaking

dx.doi.org/10.1021/jp203454g |J. Phys. Chem. C 2011, 115, 13630–13636

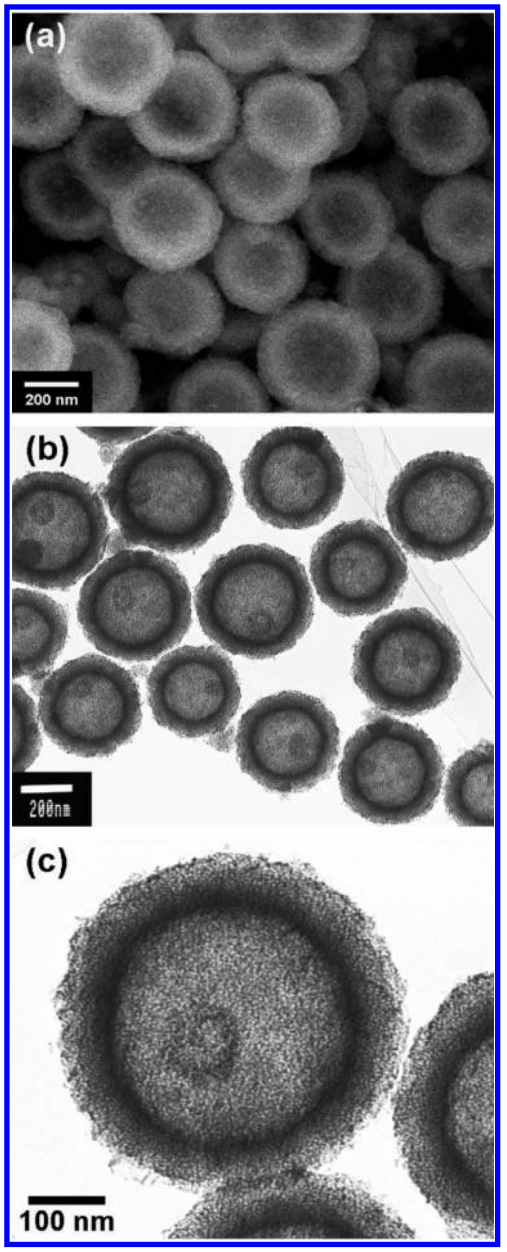

Figure 2. SEM and TEM images of hollow mesoporous silica (HMS) particles.

bed at 37 °C. Typically, 200 μg of the MFHMS/$(CpG/PLL)_3$ particles was immersed into 1 mL of α-chymotrypsin solution (10 μg/mL, 0.1 M acetic acid buffer, pH 5.6) in a 1.5 mL tube, and the tube was fixed on shaking bed with a 100 rpm of shaking speed. After a predetermined time interval, 10 μL of the suspension was removed and centrifuged, and the supernatant was used for quantitative analysis of fluorescein and CpG ODN at the wavelength of 494 and 260 nm, respectively, on a NanoDrop 2000 spectrometer.

Characterization Methods. Scanning electron microscopy (SEM) was carried out with a Hitachi S4800 field emission scanning electron microscope. Transmission electron microscopy (TEM) was performed with a JEM-2000FX electron microscope operated at an acceleration voltage of 200 kV. N_2 adsorption−desorption isotherms were obtained on a Quantachrome Autosorb 1C apparatus at −196 °C under continuous

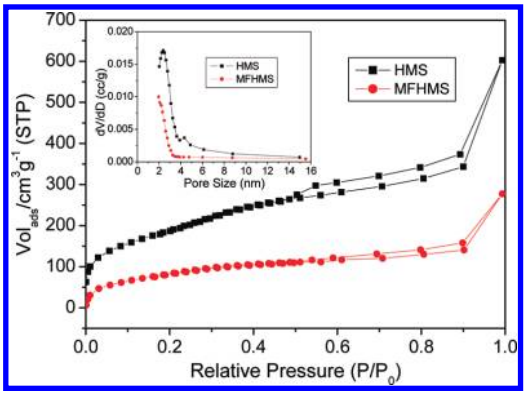

Figure 3. N_2 adsorption−desorption isotherms of the HMS and MFHMS particles and corresponding pore size distributions (inset).

Table 1. Structure Parameters of the HMS and MFHMS Particles

samples	S_{BET} (m^2/g)	V_p (cm^3/g)	D_p (nm)
HMS	688.8	0.543	2.4
MFHMS	254.4	0.164	<2

adsorption conditions. BET and BJH analyses were used to determine the surface area, the pore size distribution, and the pore volume. Zeta potential measurements were conducted on laser electrophorisis zeta-potential analyzer (LEZA-600, Otsuka, Japan). UV/vis spectra were recorded on a NanoDrop 2000 spectrometer.

RESULTS AND DISCUSSION

Characterization of HMS Particles. Figure 2 shows the SEM and TEM images of HMS particles. Similar to our previous reported results,[47−49] these particles are well monodisperse and spherical morphology. The average particle size is in the range of 300−500 nm, and the silica shell is about 70−80 nm in thickness. From the high magnification TEM image in Figure 2c, disordered mesopores are distributed on the shells. It can also be observed that one small Fe_3O_4 particle of ca. 100 nm in diameter was encapsulated in each HMS sphere. These HMS particles exhibited a ferromagnetic property with the M_s (magnetization saturation) value of 1.35 emu/g and can be targeted by an external magnetic field (see Supporting Information). Therefore, these HMS particles have potential for targeting delivery.

The N_2 adsorption−desorption isotherm of HMS particles can classified as type IV isotherm, typical curve for mesoporous materials (Figure 3). As shown in Table 1, the specific surface area was 688.8 m^2/g calculated from the linear part of the BET (Brunauer−Emmett−Teller) plot. The single point adsorption total volume at $P/P_0 = 0.90$ was 0.543 cm^3/g. The corresponding pore size distribution curve calculated from the desorption branch by the BJH (Barrett−Joyner−Halenda) method showed a narrow pore size distribution peaked at 2.4 nm, allowing small dye molecules, fluorescein, to diffuse into the hollow cavities through the mesoporous shells.

Preparation of the Fluorescein and CpG ODN-Loaded HMS/PLL Particles. Fluorescein loading and amino modification of HMS particles were characterized by UV/vis spectra, zeta potential, and N_2 adsorption−desorption measurement.

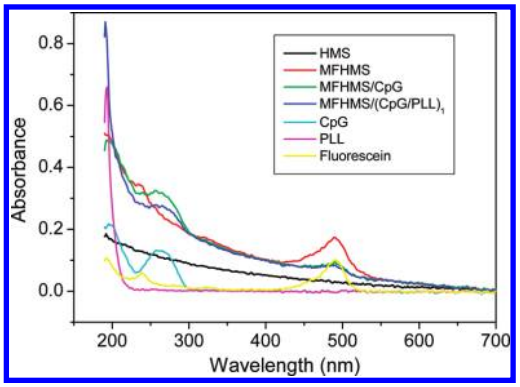

Figure 4. UV/vis spectra of the samples before and after the fluorescein and CpG ODN loading.

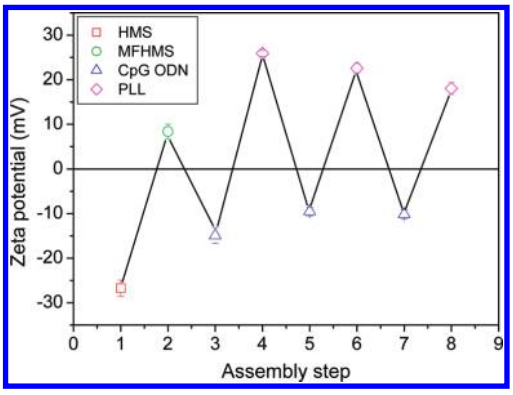

Figure 5. Zeta potential of the MFHMS/$(CpG/PLL)_n$ particles as a function of the assembly steps.

From UV/vis spectrum in Figure 4, the characteristic UV/vis absorption peak of fluorescein is found at 494 nm on the spectrum of the MFHMS sample, which suggests that fluorescein has been loaded in HMS particles. As shown in Figure 5, the zeta potential of HMS particles was −26.7 mV, while that of the MFHMS particles was 8.4 mV, which confirms the amino modification on the surface of the fluorescein-loaded HMS particles. Therefore, the MFHMS particles are able to interact with the negatively charged CpG ODN, resulting in the CpG ODN coating on the MFHMS particles. N_2 adsorption−desorption measurement further confirmed the fluorescein loading and amino modification of HMS particles (Figure 3). After the fluorescein loading and amino modification of HMS particles, the significant decreases in the N_2 volume adsorbed and specific surface area (254.4 m^2/g) were observed, which suggests a decrease of the porosity, resulting from a high content of fluorescein filling the pores and amino modification on the surface of HMS particles.

The formation of the MFHMS/$(CpG/PLL)_n$ particles was driven mainly by electrostatic interaction between negatively charged CpG ODN and positively charged PLL polymer on the MFHMS particles. The zeta potential as a function of the coating of CpG ODN and PLL polymer is shown in Figure 5. As expected, the MFHMS particles had a positive zeta potential of 8.4 mV. The coating of CpG ODN caused a reversal in zeta potential to a negative value of −14.9 mV, and subsequent coating of a positively charged PLL polymer reversed the zeta potential back to positive value, again (25.9 mV). Further coating

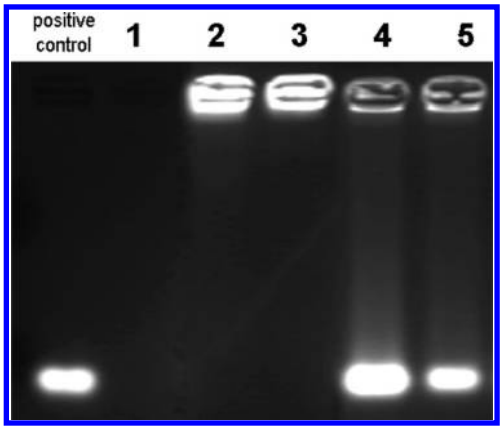

Figure 6. Gel electrophoresis of the MFHMS suspension and the MFHMS/$(CpG/PLL)_n$ suspensions before and after the treatment with an α-chymotrypsin solution: lane 1 for the MFHMS suspension; lanes 2 and 3 for the MFHMS/$(CpG/PLL)_3$ and MFHMS/$(CpG/PLL)_1$ suspensions before the α-chymotrypsin treatment, respectively; lanes 4 and 5 for the MFHMS/$(CpG/PLL)_3$ and MFHMS/$(CpG/PLL)_1$ suspensions after the α-chymotrypsin treatment for 24 h, respectively.

of CpG ODN and PLL polymer caused the zeta potential to alternate in sign, depending on whether the outermost layer was positively or negatively charged. The alternation in zeta potential qualitatively demonstrated a successful stepwise coating of CpG ODN and PLL polymer and the formation of CpG ODN/PLL multilayers on the surface of the MFHMS particles.

On the other hand, the CpG ODN loading on the MFHMS/$(CpG/PLL)_n$ particles can be determined by an agarose gel electrophoresis experiment because the positively charged MFHMS/$(CpG/PLL)_n$ particles can be retarded in gel electrophoresis, while free CpG ODN cannot be retarded.[38] As shown in Figure 6, the MFHMS particles (lane 1) have not any signal due to no CpG ODN on the particles. For the MFHMS/$(CpG/PLL)_3$ (lane 2) and MFHMS/$(CpG/PLL)_1$ (lane 3) particles, the CpG ODN was completely retained in the sample wells with no electrophoresis shift corresponding to free CpG ODN (positive control), which indicates that CpG ODN can been loaded on the MFHMS particles by a layer-by-layer assembly of CpG ODN and PLL polymer.

Also, the UV/vis spectrum further confirmed the fluorescein and CpG ODN loading on the MFHMS/$(CpG/PLL)_n$ particles. As shown in Figure 4, after CpG ODN and PLL polymer were coated on the surface of the MFHMS particles, the characteristic absorption peaks of fluorescein and CpG ODN could be observed on the UV/vis spectrum of the MFHMS/$(CpG/PLL)_1$ particles, suggesting that the MFHMS/$(CpG/PLL)_1$ particles have loaded with the fluorescein and CpG ODN.

To determine the fluorescein and CpG ODN loading capacities in the MFHMS/$(CpG/PLL)_n$ particles, UV/vis analyses at 494 nm for fluorescein and 260 nm for CpG ODN were used, respectively (Figure 7). The fluorescein loading capacity exhibited a decrease after CpG ODN coating on the MFHMS particles due to a part of fluorescein release during CpG ODN coating and then almost no decrease with the layer-by-layer assembly of PLL polymer and CpG ODN due to the capping of the openings by CpG ODN and PLL polymer. The fluorescein loading capacity of the MFHMS/$(CpG/PLL)_3$ particles was 28.8 μg/mg. The CpG ODN loading capacity increased with the increase of the assembled layers of CpG ODN, and the MFHMS/$(CpG/PLL)_3$

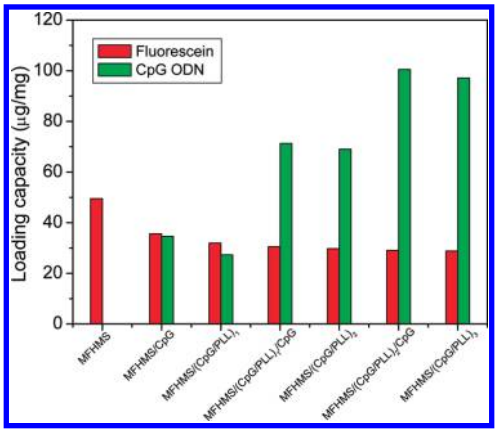

Figure 7. Fluorescein and CpG ODN loading capacities on the samples during the preparation procedure.

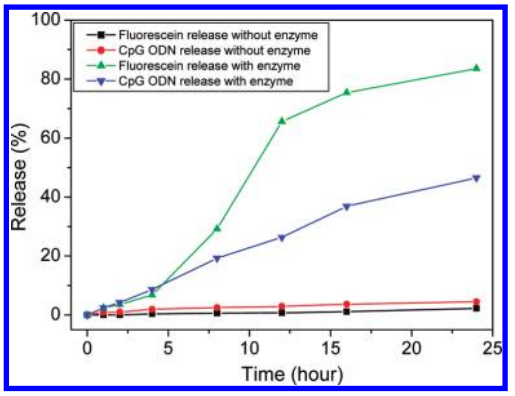

Figure 8. Release profiles of fluorescein and CpG ODN from the MFHMS/$(CpG/PLL)_3$ particles in 0.1 M acetic acid buffer in the absence and in the presence of α-chymotrypsin (10 μg/mL).

particles reached 97.1 μg/mg. Therefore, this kind of CpG ODN loading method facilitates the high loading of CpG ODN on the carriers.

***In Vitro* Release Behavior of the MFHMS/$(CpG/PLL)_n$ Particles.** To investigate the enzyme-triggered release of fluorescein and CpG ODN from the MFHMS/$(CpG/PLL)_n$ particles, α-chymotrypsin was used as a model enzyme for enzymatic degradation of PLL polymer layers. The MFHMS/$(CpG/PLL)_3$ and MFHMS/$(CpG/PLL)_1$ particles were treated with an α-chymotrypsin solution (10 μg/mL) in 0.1 M acetic acid buffer (pH 5.6) at 37 °C for 24 h, and the suspensions were used for agarose gel electrophoresis experiment. As shown in Figure 6, the α-chymotrypsin-treated MFHMS/$(CpG/PLL)_3$ (lane 4) and MFHMS/$(CpG/PLL)_1$ (lane 5) suspensions showed the electrophoresis shift corresponding to free CpG ODN. This suggests that CpG ODN can release from the MFHMS/$(CpG/PLL)_n$ particles by the treatment of α-chymotrypsin solution for enzymatic degradation of PLL polymer layers.

Figure 8 shows the release behaviors of fluorescein and CpG ODN from the MFHMS/$(CpG/PLL)_3$ particles in the absence and in the presence of α-chymotrypsin. The MFHMS/$(CpG/PLL)_3$ particles exhibited a negligible release of fluorescein and CpG ODN in the absence of α-chymotrypsin, thus indicating that CpG ODN was immobilized on PLL layers and CpG/PLL layers tightly capped the openings of mesopores. In contrast,

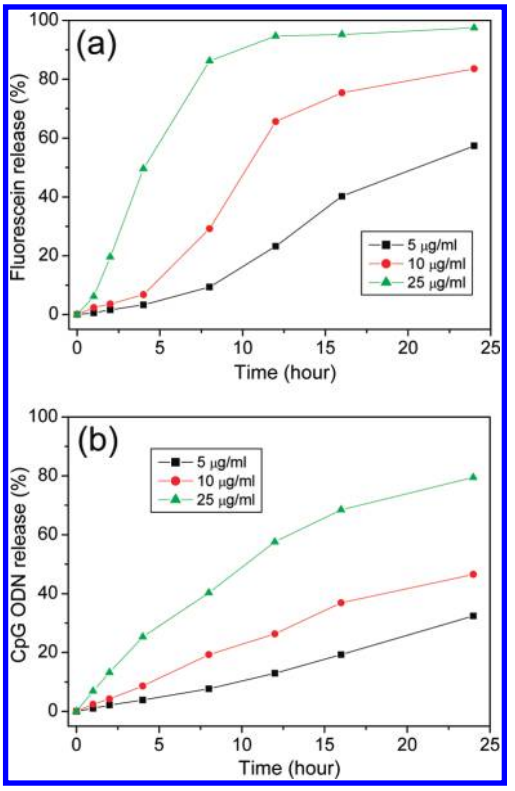

Figure 9. Release profiles of fluorescein (a) and CpG ODN (b) from the MFHMS/$(CpG/PLL)_3$ particles in the α-chymotrypsin solutions with different concentrations.

the presence of α-chymotrypsin induced fluorescein and CpG ODN release from the MFHMS/$(CpG/PLL)_3$ particles. After the MFHMS/$(CpG/PLL)_3$ particles were added into an α-chymotrypsin solution (10 μg/mL) at 37 °C, CpG ODN was released from PLL layers by the enzymatic degradation of the PLL layers, and ~45% of the loaded CpG ODN was released after 24 h. Meanwhile, the fluorescein was also released from the MFHMS/$(CpG/PLL)_3$ particles due to the uncapping of the openings during the degradation of the PLL layers and the release of CpG ODN. Interestingly, the fluorescein release curve shows a relatively slow release for the early stage, followed by a fast release. It may be explained that the slow degradation of PLL layers in the early stage led to few uncapped openings, and few fluorescein molecules can release from the particles. With increasing the degradation time of PLL layers, an increasing number of openings were uncapped, resulting in more fluorescein molecules diffused out of the HMFHMS particles.

Furthermore, the release rate of fluorescein and CpG ODN can be controlled by changing the concentration of the α-chymotrypsin solution. As shown in Figure 9, the release rates of fluorescein and CpG ODN increased with the increase of the α-chymotrypsin concentrations. The release of CpG ODN and fluorescein depends on the enzymatic degradation of PLL layers. The higher α-chymotrypsin concentration led to the faster degradation rate of PLL layers and induced a faster release of CpG ODN. Meanwhile, more openings of mesopores could be uncapped for fluorescein release, resulting in the increased fluorescein release rate. Therefore, the MFHMS/$(CpG/PLL)_3$ particles have an enzyme-triggered controlled release property.

CONCLUSION

We proposed a concept to design an enzyme-triggered drug and gene codelivery system by the formation of HMS/PLL particles driven by electrostatic interaction between negatively charged gene and positively charged PLL polymer on the drug-loaded HMS particles. HMS particles provided high drug loading capacity; the coating of gene/PLL layer on the drug-loaded HMS particles via the layer-by-layer assembly could cap the openings of mesopores and load gene. This codelivery system can give an enzyme-triggered controlled release of drug and gene simultaneously, and the release rates of drug and gene from the HMS/PLL particles can also be controlled by changing the enzyme concentration. Therefore, this system has the advantages of both enzyme-triggered controlled release and codelivery of drug and gene and would have potential and promising applications in the field of biomedicine and cancer therapy.

ASSOCIATED CONTENT

Supporting Information. Preparation of hollow mesoporous silica particles, gel electrophoresis and UV/vis spectra measurements, and the magnetic property of HMS particles. This material is available free of charge via the Internet at http://pubs.acs.org.

AUTHOR INFORMATION

Corresponding Author
*Tel +86-21-55271663; e-mail zjf2412@163.com.

ACKNOWLEDGMENT

The authors gratefully acknowledge the support provided by Shanghai Pujiang Program, the Opening Project of State Key Laboratory of High Performance Ceramics and Superfine Microstructure (No. SKL201004SIC) and the Starting Fund from University of Shanghai for Science and Technology (No. 10-00-310-001).

REFERENCES

(1) Vivero-Escoto, J. L.; Slowing, I. I.; Trewyn, B. G.; Lin, V. S.-Y. *Small* **2010**, *6*, 1952–1967.
(2) Manzano, M.; Vallet-Regí, M. *J. Mater. Chem.* **2010**, *20* 5593–5604.
(3) Hudson, S.; Cooney, J.; Magner, E. *Angew. Chem., Int. Ed.* **2008**, *47*, 2–15.
(4) Hom, C.; Lu, J.; Tamanoi, F. *J. Mater. Chem.* **2009**, *19* 6308–6316.
(5) Liu, R.; Zhang, Y.; Zhao, X.; Agarwal, A.; Mueller, L. J.; Feng, P. *J. Am. Chem. Soc.* **2010**, *132*, 1500–1501.
(6) Giri, S.; Trewyn, B. G.; Stellmaker, M. P.; Lin, V. S.-Y. *Angew. Chem., Int. Ed.* **2005**, *44*, 5038–5044.
(7) Lai, C. Y.; Trewyn, B. G.; Jeftinija, D. M.; Jeftinija, K.; Xu, S.; Jeftinija, S.; Lin, V. S.-Y. *J. Am. Chem. Soc.* **2003**, *125*, 4451–4459.
(8) Luo, Z.; Cai, K.; Hu, Y.; Zhao, L.; Liu, P.; Duan, L.; Yang, W. *Angew. Chem., Int. Ed.* **2011**, *50*, 640–643.
(9) Climent, E.; Martínez-Máñez, R.; Sancenón, F.; Marcos, M. D.; Soto, J.; Maquieira, A.; Amorós, P. *Angew. Chem., Int. Ed.* **2010**, *49* 7281–7283.
(10) Chen, C.; Geng, J.; Pu, F.; Yang, X.; Ren, J.; Qu, X. *Angew. Chem., Int. Ed.* **2011**, *50*, 882–886.
(11) Climent, E.; Bernardos, A.; Martínez-Máñez, R.; Maquieira, A.; Marcos, M. D.; Pastor-Navarro, N.; Puchades, R.; Sancenón, F.; Soto, J.; Amorós, P. *J. Am. Chem. Soc.* **2009**, *131*, 14075–14080.
(12) Casasús, R.; Climent, E.; Marcos, M. D.; Martínez-Máñez, R.; Sancenón, F.; Soto, J.; Amorós, P.; Cano, J.; Ruiz, E. *J. Am. Chem. Soc.* **2008**, *130*, 1903–1917.
(13) Zhu, Y.; Shi, J.; Shen, W.; Dong, X.; Feng, J.; Ruan, M.; Li, Y. *Angew. Chem., Int. Ed.* **2005**, *44*, 5083–5087.
(14) Mal, N. K.; Fujiwara, M.; Tanaka, Y. *Nature* **2003**, *421* 350–353.
(15) Kim, T. W.; Slowing, I. I.; Chung, P.-W.; Lin, V. S.-Y. *ACS Nano* **2011**, *5*, 360–366.
(16) Coll, C.; Casasús, R.; Aznar, E.; Marcos, M. D.; Martínez-Máñez, R.; Sancenón, F.; Soto, J.; Amorós, P. *Chem. Commun.* **2007** 1957–1959.
(17) Lee, C.-H.; Cheng, S.-H.; Huang, I. P.; Souris, J. S.; Yang, C.-S.; Mou, C.-Y.; Lo, L.-W. *Angew. Chem., Int. Ed.* **2010**, *49*, 8214–8219.
(18) Chang, M.-W.; Stride, E.; Edirisinghe, M. *J. R. Soc. Interface* **2011**, *8*, 451–456.
(19) Thornton, P. D.; Mart, R. J.; Webb, S. J.; Ulijn, R. V. *Soft Matter* **2008**, *4*, 821–827.
(20) Itoh, Y.; Matsusaki, M.; Kida, T.; Akashi, M. *Biomacromolecules* **2006**, *7*, 2715–2718.
(21) De Geest, B. G.; Vandenbroucke, R. E.; Guenther, A. M.; Sukhorukov, G. B.; Hennink, W. E.; Sanders, N. N.; Demeester, J.; De Smedt, S. C. *Adv. Mater.* **2006**, *18*, 1005–1009.
(22) Orozco, V. H.; Kozlovskaya, V.; Kharlampieva, E.; Lopez, B. L.; Tsukruk, V. V. *Polymer* **2010**, *51*, 4127–4139.
(23) Patel, K.; Angelos, S.; Dichtel, W. R.; Coskun, A.; Yang, Y.-W.; Zink, J. I.; Stoddart, J. F. *J. Am. Chem. Soc.* **2008**, *130*, 2382–2383.
(24) Park, C.; Kim, H.; Kim, S.; Kim, C. *J. Am. Chem. Soc.* **2009**, *131*, 16614–16615.
(25) Bernardos, A.; Aznar, E.; Marcos, M. D.; Martínez-Máñez, R.; Sancenón, F.; Soto, J.; Barat, J. M.; Amorós, P. *Angew. Chem., Int. Ed.* **2009**, *48*, 5884–5887.
(26) Schlossbauer, A.; Kecht, J.; Bein, T. *Angew. Chem., Int. Ed.* **2009**, *48*, 3092–3095.
(27) Thornton, P. D.; Heise, A. *J. Am. Chem. Soc.* **2010**, *132* 2024–2028.
(28) Bernardos, A.; Mondragon, L.; Aznar, E.; Marcos, M. D.; Martínez-Máñez, R.; Sancenón, F.; Soto, J.; Barat, J. M.; Perez-Paya, E.; Guillem, C.; Amorós, P. *ACS Nano* **2010**, *4*, 6353–6368.
(29) Cotton, M.; Wagner, E.; Zatloukal, K.; Phillips, S.; Curiel, D. T.; Birnstiel, M. L. *Proc. Natl. Acad. Sci. U.S.A.* **1992**, *89* 6094–6098.
(30) Kishida, T.; Asada, H.; Itokawa, Y.; Yasutomi, K.; Shinya, M.; Gojo, S.; Cui, F.-D.; Ueda, Y.; Yamagishi, H.; Imanishi, J.; Mazda, O. *Mol. Ther.* **2003**, *8*, 738–745.
(31) Liu, F.; Shollenberger, L. M.; Huang, L. *FASEB J.* **2004**, *18*, 1779–1781.
(32) Lee, A. L. Z.; Wang, Y.; Cheng, H. Y.; Pervaiz, S.; Yang, Y. Y. *Biomaterials* **2009**, *30*, 919–927.
(33) Wang, Y.; Gao, S.; Ye, W.-H.; Yoon, H. S.; Yang, Y.-Y. *Nature Mater.* **2006**, *5*, 791–796.
(34) Xu, Z.; Zhang, Z.; Chen, Y.; Chen, L.; Lin, L.; Li, Y. *Biomaterials* **2010**, *31*, 916–922.
(35) Mizuno, Y.; Naoi, T.; Nishikawa, M.; Rattanakiat, S.; Hamaguchi, N.; Hashida, M.; Takakura, Y. *J. Controlled Release* **2010**, *141*, 252–259.
(36) Zhang, L.; Lu, Z.; Zhao, Q.; Huang, J.; Shen, H.; Zhang, Z. *Small* **2011**, *7*, 460–464.
(37) Torney, F.; Trewyn, B. G.; Lin, V. S.-Y.; Wang, K. *Nature Nanotechnol.* **2007**, *2*, 295–300.
(38) Chen, A. M.; Zhang, M.; Wei, D.; Stueber, D.; Taratula, O.; Minko, T.; He, H. *Small* **2009**, *5*, 2673–2677.
(39) Zhu, Y.; Shi, J.; Shen, W.; Chen, H.; Dong, X.; Ruan, M. *Nanotechnology* **2005**, *16*, 2633–2638.
(40) Feng, Z.; Li, Y.; Niu, D.; Li, L.; Zhao, W.; Chen, H.; Li, L.; Gao, J.; Ruan, M.; Shi, J. *Chem. Commun.* **2008**, *23*, 2629–2631.
(41) Wang, J. G.; Li, F.; Zhou, H.-J.; Sun, P.-C.; Ding, D.-T.; Chen, T.-H. *Chem. Mater.* **2009**, *21*, 612–620.

(42) Chang, M.-W.; Stride, E.; Edirisinghe, M. *Langmuir* **2010**, *26*, 5115–5121.
(43) Zhang, X.; Oulad-Abdelghani, M.; Zelkin, A. N.; Wang, Y.; Haikel, Y.; Mainard, D.; Voegel, J.-C.; Caruso, F.; Benkirane-Jessel, N. *Biomaterials* **2010**, *31*, 1699–1706.
(44) Incani, V.; Lin, X.; Lavasanifar, A.; Uludag, H. *ACS Appl. Mater. Interfaces* **2009**, *1*, 841–848.
(45) Itoh, Y.; Matsusaki, M.; Kida, T.; Akashi, M. *Chem. Lett.* **2008**, *37*, 238–239.
(46) Wang, Z.; Qian, L.; Wang, X.; Zhu, H.; Yang, F.; Yang, X. *Colloids Surf., A* **2009**, *332*, 164–171.
(47) Zhu, Y.; Kockrick, E.; Ikoma, T.; Hanagata, N.; Kaskel, S. *Chem. Mater.* **2009**, *21*, 2547–2553.
(48) Zhu, Y.; Ikoma, T.; Hanagata, N.; Kaskel, S. *Small* **2010**, *6* 471–478.
(49) Zhu, Y.; Fang, Y.; Kaskel, S. *J. Phys. Chem. C* **2010**, *114* 16382–16388.